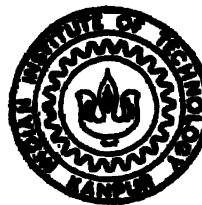


9270103

# FLIGHT PATH CONTROL THROUGH THE AIRBRAKES DURING THE LANDING APPROACH

by

**ASHISH BALAYA**



TH  
629.1321213  
B184f

Th.  
AE/1994/M.  
B184f

AE  
1994  
M  
BAL  
FLI

DEPARTMENT OF AEROSPACE ENGINEERING  
INDIAN INSTITUTE OF TECHNOLOGY KANPUR  
March 1994

**FLIGHT PATH CONTROL THROUGH THE AIRBRAKES  
DURING THE LANDING APPROACH**

*A thesis submitted in partial fulfillment of the requirements for  
the degree of Master of Technology*

*by*

**ASHISH BALAYA**

**DEPT. OF AEROSPACE ENGINEERING.**

**I . I . T . Kanpur**

13 APR 1994  
117672

AE-1994-M-BAL-FLI

CERTIFICATE

16.3.94  
D<sub>2</sub> /

It is certified that the work contained in this thesis entitled "Flight Path Control through the Airbrakes during the Landing Approach" by Ashish Balaya has been carried out under my supervision and that this work has not been submitted elsewhere for a degree.

*Krishna Kumar*

Signature of the Supervisor :

Name : Dr. Krishna Kumar

March, 1994

Department : Aerospace Engineering

I. I. T. Kanpur

## ABSTRACT

Fighter aircraft often encounter handling difficulties during the crucial approach phase of the landing maneuver. This manifests itself as a significant dip in the flight path angle before settling to the desired command levels. This abnormal trend can generate considerable confusion in the pilot during this vital flight phase. At present, the pilots attempt to cope with this airplane behavior by constant juggling between the throttle and the stick. It may be pointed out that this pilot maneuver is rather demanding, especially in view of the large lags in the response of the engine.

In the present investigation an attempt has been made to understand the root cause of the problem through a parametric study. The study suggests that the presence, in the right half s-plane, of the zero  $(-1/T_{h1})$  in the flight path angle - to - elevator transfer function, brings about the undesirable flight path response during landing approach.

Next an attempt has been made to synthesise a MIMO control system utilising the airbrakes, in order to ensure that this zero stays in the left half s - plane. A classical approach to MIMO systems is adapted to the design problem at hand. This approach utilises the closure of the feedback loops in a sequential manner. It also allows for the placement of the poles as well as the zeros of the transfer function of interest by a simple root locus design procedure.

The results clearly demonstrate the efficacy of the proposed autopilot in overcoming the problem of the flight path dip during the landing phase as well as statically decoupling the airspeed from the flight path.

For Shiboo, my fiancée,  
who walked into my life so suddenly;  
and stoically bore all my absences  
when I was slogging away.

## ACKNOWLEDGEMENTS

At the outset I wish to thank my guide, Dr. Krishna Kumar, for the stimulating environment he created, in which I had the freedom to try innovative ideas of my own, in the secure knowledge that they would be judged largely on the basis of their merit and soundness and not just by the yardstick of established practice.

It is with sincere gratitude that I want to thank Dr. S.C.Raisinghani for planting the germ of the idea of the airbrakes into my mind. This is what is mainly responsible for the birth and subsequent evolution of this thesis.

Special thanks to Prof. C.V.R.Murti for guiding me through the maze of flight path dynamics by a series of interesting discussions which threw a lot of light upon the problem of interest.

I fail to imagine what my days at IIT-K would be without the constant (except when he was in one of his phases) companionship of Neeraj, who proved a virtually endless source of fun in the form of all-night discussions or just sitting around listening to our favourite music. I also "hold him responsible" for introducing me to jazz and his "heh-heh" and special style of enunciation will remain in my psychic residues long after my body has turned to dust.



I would feel terribly guilty if I went any further down this list without mentioning Siva the Great. Its very unfortunate that his help falls in the category of "CLASSIFIED" information but he knows what he did for me and I do; and between the two of us, that's enough. Right, Siva?

Soma and Mukku, thanks for all that you guys did for me back at home. Ravi and Indu, thanks for keeping the tension alive in me with your news and views of life.

The long walks and discussions with G.K., on the topic of Flight Controls, a passion with both of us, will ever serve to remind me that even now, in a world rife with software engineers, there are people who stick to more interesting activities like designing flight control systems. Yeah, yeah, G.K.

And then there's the gang of Ajju, Ranki, Kak, Rogers and, how could I forget, Pikkoo who were always there with the spirit of cheer when I needed it. Thanks to all of them. Keep juggling, Ranki.

I'll end with the one special personality who literally kept me awake during the nights and thus forced me to work even when I wanted to sleep. Thanks, Tintin, I wish I could tell you how much you came to mean to me in this couple of years. But I guess you already know, in that special way that only dogs have.

## **CONTENTS**

<b>CHAPTER 1 : INTRODUCTION</b>	<b>Pg. 1</b>
<b>CHAPTER 2 : PROBLEM ANALYSIS</b>	<b>Pg. 4</b>
<b>CHAPTER 3 : CONTROLLER SYNTHESIS</b>	<b>Pg. 15</b>
<b>CHAPTER 4 : RESULTS AND CONCLUSIONS</b>	<b>Pg. 37</b>

## LIST OF FIGURES

FIGURE 1 : Typical Flight Path Response to an elevator step input	Pg. 7
FIGURE 2 : General Structure of a Multi-loop Flight Control System	Pg. 16
FIGURE 3 : Equivalent Block Diagram of the System : $X_1 \rightarrow \delta_1$ ; $X_2 \rightarrow \delta_2$	Pg. 20
FIGURE 4 : Equivalent Subsystems of the System : $X_2 \rightarrow \delta_2$	Pg. 21
FIGURE 5 : Root Locus of the Coupling Loop B	Pg. 26
FIGURE 6 : Root Locus of the Coupling Loop B with the lead compensator	Pg. 27
FIGURE 7 : Root Locus of the Inner Loop A with the lead compensator	Pg. 29
FIGURE 8 : Root Locus of the outer Flight Path Loop.	Pg. 31
FIGURE 9 : Flight Path Response to Flight Path Command (no compensator)	Pg. 32
FIGURE 10 : Airspeed Response to Flight Path Command (no compensator)	Pg. 33
FIGURE 11 : Flight Path Response to Flight Path Command (with compensator)	Pg. 35
FIGURE 12 : Airspeed response to Flight Path Command (with compensator)	Pg. 36

## LIST OF TABLES

TABLE 1	: Results of the Parameter-study	Pg. 10
TABLE 1(a)	: Results of the Parameter-study (contd)	Pg. 12

## CHAPTER 1

### INTRODUCTION

The landing approach represents a rather important phase in an airplane flight mission. The successful completion of the mission requires much greater precision in airplane handling during this crucial phase. The importance of this becomes evident from the large number of failures and associated loss of life that may be attributed to inadequate flying qualities during this terminal phase.

The acceptable handling qualities for the approach phase demand control over two flight parameters -- the forward airspeed as well as the rate of descent. The pilot's handling task involved here is particularly more demanding because of the coupling invariably present between the vertical sink rate and the airspeed. Evidently, this significantly adds to the pilot's workload. Needless to say, in the present era of modern high performance airplanes there is little scope for pilot error even in the face of such excessive demands, more so in this terminal phase.

For the twin control of the sink rate and the airspeed, only a single aerodynamic surface is available - the elevator. The use of the throttle enables the airplane designer to provide for the second control normally needed. To achieve proper coordination

between these two flight parameters the pilot makes use of the throttle on an as-and-when-needed basis. Fortunately this control function does not normally involve lateral directional control actuation.

In general, it is easy to ensure successful airplane handling in non-terminal phases; however, during the landing approach, there being excessive time lag in the throttle response, difficulties are encountered. One can only imagine the problems while landing upon an aircraft carrier at sea, especially during a storm. Hence providing the pilot with a suitable control mechanism without such a time lag problem appears to be a must. Even during the less critical phases it would be worthwhile to have dual simultaneous control over the rate of descent and the airspeed to reduce the pilot's overall workload and thus indirectly enhance mission success rates.

The present controller designs [1,2] centre around the idea of using feedback actuation of the throttle and the elevator simultaneously. These systems suffer from the throttle time-lag problem. Besides, the thrust needs to be adjusted to re-establish equilibrium each time there is a disturbance or when the pilot wants to change either of the two flight parameters. This causes the wear and tear of the power plant to increase significantly [2]. Thus, for better handling and reduced engine wear, an alternative actuation system is required in the longitudinal channel.

The airbrake is selected here to provide for the additional control surface. It may seem an unconventional choice, but it offers several advantages over the throttle (2). Firstly, the control being exercised through an aerodynamic surface, it hardly suffers from the time-lag problem associated with the throttle. Secondly, it reduces the wear and tear on the engine, now operating at a constant throttle setting. Finally, since the airbrake is deployed, the throttle setting is going to be higher than it would be during a conventional landing. That turns out to be an added advantage for a sudden abortion of landing -- if forced -- as the pilot can simply retract the airbrake to get an almost instantaneous boost in the airspeed. The go-around is further facilitated through faster engine response by virtue of the higher throttle setting now in operation. It is felt that these advantages may make the airbrake a particularly attractive choice for the design of the flight path controller for the approach phase of the modern high performance fighter airplanes.

## CHAPTER 2 PROBLEM ANALYSIS

For a better assessment of the problem of regulating the flight path during approach, it is desirable to develop a clear understanding of the various terms involved in the governing transfer function of the airplane. This would enable us to identify the more important system parameters and hence the associated stability derivatives.

We therefore carefully examine a typical transfer function for a fighter aircraft during the terminal phase under consideration [3]:

$$\frac{\gamma(s)}{\delta_e(s)} = \frac{k\gamma (s + 1/T_{h1})(s + 1/T_{h2})(s + 1/T_{h3})}{[s^2 + 2\zeta_{sp}\omega_{sp}s + \omega_{sp}^2][s^2 + 2\zeta_{ph}\omega_{ph}s + \omega_{ph}^2]}$$

where

$\gamma$  = flight path angle (rad)

$\delta_e$  = elevator deflection (rad)

$s$  = Laplacian variable

$k\gamma$  = constant gain factor

$\zeta_{sp}$  = short period damping ratio

$\omega_{sp}$  = short period natural frequency (rad/s)

$\zeta_{ph}$  = phugoid damping factor

$\omega_{ph}$  = phugoid natural frequency (rad/s)

$(1/T_{h1})$ ,  $(1/T_{h2})$  and  $(1/T_{h3})$  are numerator time constants with

i)  $T_{h1} > 0$  and  $T_{h2} = 0$

ii)  $|T_{h1}| > |T_{h2}|$  or  $|T_{h3}|$



It is evident that the above transfer function has :

- i) zeros at  $(-1/T_{h1}), (-1/T_{h2}), (-1/T_{h3})$
- ii) poles at  $[{-\zeta_{sp} \pm \sqrt{1-\zeta_{sp}^2}}] \cdot \omega_{sp}$  and  $[{-\zeta_{ph} \pm \sqrt{1-\zeta_{ph}^2}}] \cdot \omega_{ph}$

The importance of these s-plane locations cannot be over emphasised since the airplane flight path response during any flight phase is dictated by their instantaneous values. As is well known, the above parameters undergo significant variations as the airplane goes through changes of flight regime and maneuvers.

It is found that increasing the Mach number causes the two extreme zeros ( $-1/T_{h2}$  and  $-1/T_{h3}$ ) to drift further apart while the third, ( $-1/T_{h1}$ ), lying between these two and rather close to the imaginary axis, moves to the left. Inversely, during the critical phase of approach, when Mach numbers are low, this middle zero shifts to the right, getting invariably pushed even into the right-half plane. This appears to be at the root of the control problem. This fact can be better illustrated through the example given below.

**Example :** Typical data for a fighter configuration :

mass	= 9000 kg	length	= 12 m
wing area	= 40 sq m	m.a.c.	= 7 m
flight condition : Sea level, $M = 0.2$ , $\gamma = -2$ deg			

$$\frac{\gamma(s)}{\delta_e(s)} = \frac{0.1453(s - 0.0852)(s + 4.2226)(s - 2.2964)}{[s^2 + 2(0.88)(1.36)s + (1.36)^2][s^2 + 2(0.11)(0.16)s + (0.16)^2]}$$

The flight path response to a step elevator input is shown in Fig.1. The first thing that can be noticed from the response is that it exhibits a non-minimum phase behaviour i.e., the flight path angle first dips to one side and then settles at a value of the opposite sign. This, in itself, is sufficient to cause serious problems in airplane handling since the pilot feels "out of phase" with the airplane. The second important thing to be noted is that a positive elevator input causes a positive steady state value of flight path. This has obvious undesirable flying implications as now pushing forward on the pilot's stick causes the airplane to settle in a steady climb - in direct contrast to the mind-set of the pilot for the other flight phases at higher Mach numbers. Evidently this can lead to situations of confusion and occasionally even disaster. For an understanding of this observed behaviour during the approach phase, we consider the transfer function in a more convenient form :

$$\frac{\gamma(s)}{\delta_e(s)} = \frac{(s + a).(s + b).(s + c)}{[s^2 + ps + q].[s^2 + ls + m]}$$

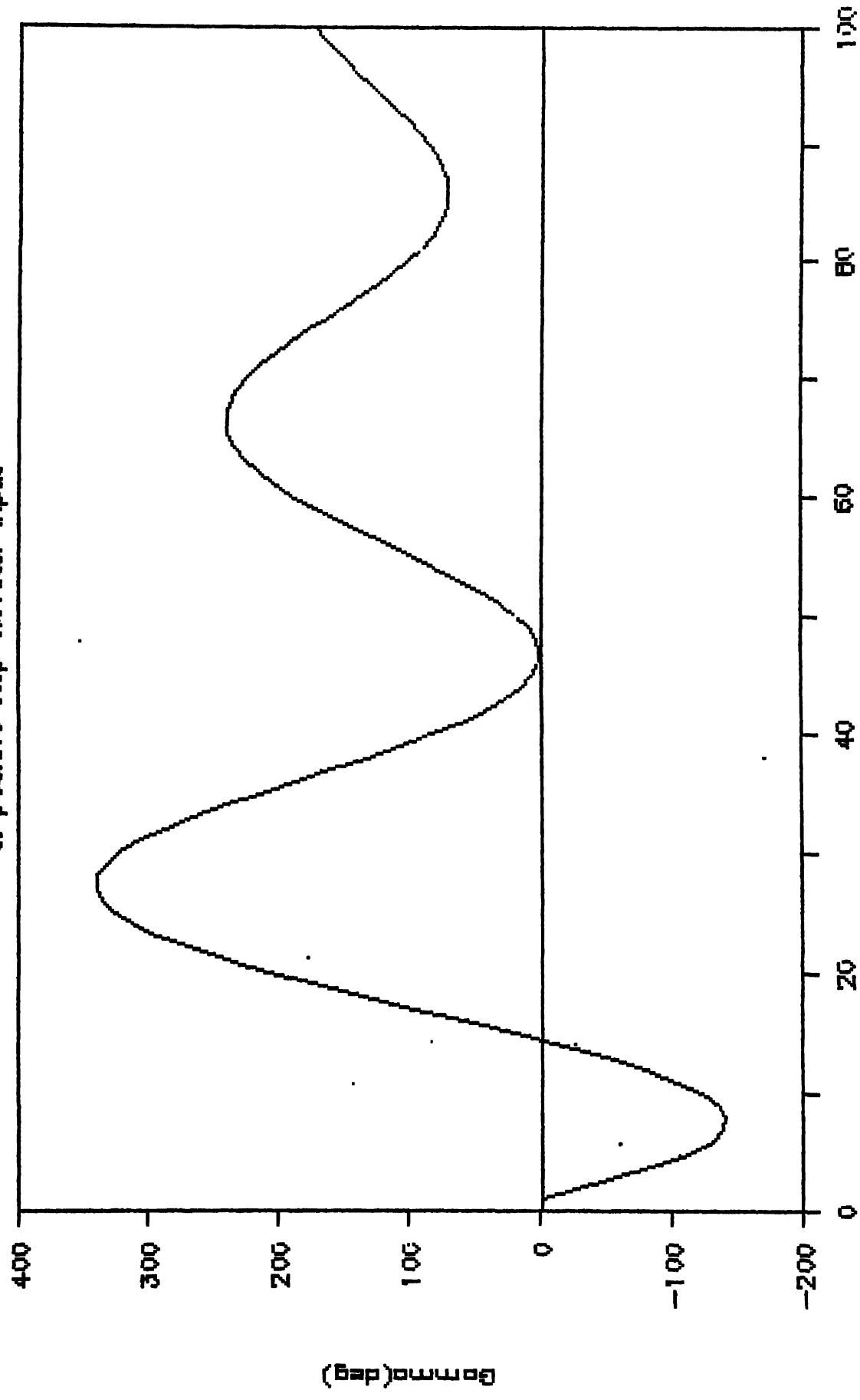
where :

$$a = 1/T_{h1}$$

$$b = 1/T_{h2}$$

$$c = 1/T_{h3}$$

Fig. 1 Typical Flight Path response  
to positive step elevator input



$$p = 2\zeta_{sp} \omega_{sp}$$

$$q = \omega_{sp}^2$$

$$l = 2\zeta_{ph} \omega_{ph}$$

$$m = \omega_{ph}^2$$

Note that  $k_T$  is taken equal to 1 for simplicity, however it has no implications as regards the validity of the analysis whatsoever.

It may be repeated that the overall flight path response depends upon the above parameter values as well as initial conditions. However, for the purpose of analysis, we assume initial conditions to be zero. This would enable us to highlight the intrinsic behaviour under the influence of the important parameters. Again, focusing upon the same objective, we take the poles, which characterise the airplane short period and phugoid modes, to be fixed while the zeros are varied.

There being three variable parameters  $a, b$  and  $c$ , these are varied one at a time while the other two are kept constant. Furthermore, since experience shows that the two extreme zeros ( $-1/T_{h2}$  and  $-1/T_{h3}$ ) move apart in unison, the number of parameters gets effectively reduced to only two --  $a$  and  $b$  (or  $c$ ).

It is interesting to point out that to examine the changes in the nature of the response, it is not necessary to solve the governing differential equation for the flight path. In fact it would suffice to break the transfer function into partial

fractions in the form

$$\frac{\gamma(s)}{\delta_{\theta}(s)} = \frac{A.(s+B)}{[s^2 + ps + q]} + \frac{C(s+D)}{[s^2 + ls + m]}$$

and simply focus upon the nature of the constants A,B,C and D and study how they change when the parameters a,b and c are varied. Needless to say, relatively large changes in the values of these constants would indicate sudden changes in the nature of response. The same could be concluded from sudden changes in the signs of the constants. Of the two modes, the phugoid being more important for the flight path, the associated constants C and D require closer scrutiny.

#### Results of the Parameter - Study :

The study undertaken here shows that of the three zeros, the one at  $(-1/T_{h1})$  is the most significant one as the changes in its value can bring about radical changes in the nature of the longitudinal response. Of the two modes, however, it is the phugoid which suffers more drastic behavioural changes while the short period one remains virtually unaffected.

Table 1 shows the results of the parameter - study. In the first part, the constant  $(1/T_{h1})$  is varied from -0.5 to +0.5, the total variation being 1250% around its nominal value, while the other two parameters  $(1/T_{h2})$  and  $(1/T_{hs})$  are held constant at their nominal values of -2.3 and +4.2 respectively.

TABLE 1.  
RESULTS OF THE PARAMETER STUDY

$\gamma / \delta_0$ Numerator (s+a)(s+b)(s+c)	Short Period Numerator A(s + B)	Plagoid Numerator C(s + D)
(s+4.2)(s-2.3)(s-0.5)	10.20(s + 2.64)	-9.28(s - 0.25)
(s+4.2)(s-2.3)(s-0.2)	7.91(s + 2.17)	-6.91(s - 0.12)
(s+4.2)(s-2.3)(s-0.1)	7.12(s + 2.23)	-6.12(s - 0.05)
(s+4.2)(s-2.3)(s-0.08)	6.86(s + 2.25)	-5.86(s - 0.03)
(s+4.2)(s-2.3)(s-0.05)	6.72(s + 2.27)	-5.72(s - 0.01)
(s+4.2)(s-2.3)(s)	6.73(s + 2.31)	-5.33(s + 0.04)
(s+4.2)(s-2.3)(s+0.05)	5.93(s + 2.35)	-4.93(s + 0.07)
(s+4.2)(s-2.3)(s+0.08)	5.69(s + 2.39)	-4.69(s + 0.13)
(s+4.2)(s-2.3)(s+0.1)	5.54(s + 2.42)	-4.54(s + 0.16)
(s+4.2)(s-2.3)(s+0.2)	4.74(s + 2.55)	-3.74(s + 0.32)
(s+4.2)(s-2.3)(s+0.5)	2.37(s + 3.51)	-1.37(s + 1.19)

To study the effect of varying the constant  $(1/T_{h1})$  upon the nature of the two longitudinal modes we compute the extent of variations in the values of the zeros of the two modes about their nominal values. It is found that the zero of the short period mode varies only 65% around nominal while the phugoid zero varies 2175% around nominal. Furthermore, the sign of  $(1/T_{h1})$  is of special significance here as it dictates the very nature of the phugoid mode. For the case  $(1/T_{h1}) = 0$ , the phugoid mode exhibits a non-minimum phase behaviour which is characterized by a zero in the right-half plane. On the other hand, when  $(1/T_{h1}) > 0$ , this abnormality disappears.

Next, we focus on studying the influence of varying the terms  $(1/T_{h2})$  and  $(1/T_{h3})$ . It may be added that the variations of these two zeros happen to have symmetry around the imaginary axis as they move apart. The term  $(1/T_{h1})$  is now held constant at its nominal value of -0.08.

In this case, partial fraction decomposition shows that except for a variation in the constant gain, the 'nature' of neither mode changes significantly for the zeros remain virtually unchanged. As a result, merely their steady state values undergo variations.

In the final phase, the effect of varying the constants  $(1/T_{h2})$  and  $(1/T_{h3})$  is examined when the sign of  $(1/T_{h1})$  is reversed. Interestingly, the tracks of the longitudinal response

**TABLE 1. (contd.)**  
**RESULTS OF THE PARAMETER STUDY**

$\gamma / \delta$ Numerator (s+a)(s+b)(s+c)	Short Period Numerator A(s + B)	Pingoid Numerator C(s + D)
(s-0.08)(s+4.2)(s-2.3)	8.98(s + 2.25)	-5.98(s - 0.03)
(s-0.08)(s+5.0)(s-3.0)	10.20(s + 2.28)	-9.20(s - 0.04)
(s-0.08)(s+8.0)(s-6.0)	30.22(s + 2.20)	-29.22(s - 0.04)
(s-0.08)(s+10.0)(s-9.0)	55.65(s + 2.29)	-54.65(s - 0.04)
(s-0.08)(s+12.0)(s-12.0)	88.36(s + 2.31)	-87.36(s - 0.04)
(s+0.08)(s+4.2)(s-2.3)	5.98(s + 2.38)	-4.69(s + 0.13)
(s+0.08)(s+5.0)(s-3.0)	8.32(s + 2.43)	-7.32(s + 0.13)
(s+0.08)(s+8.0)(s-6.0)	24.59(s + 2.45)	-23.59(s + 0.12)
(s+0.08)(s+10.0)(s-9.0)	45.33(s + 2.46)	-44.33(s + 0.12)
(s+0.08)(s+12.0)(s-12.0)	71.99(s + 2.46)	-70.99(s + 0.12)



observed earlier remain unchanged.

Thus it may be concluded that it is the sign as well as the magnitude of  $(1/T_{h1})$  that really decides the nature of the phugoid mode. This mode being more important to the flight path response, we arrive at a general and rather far-reaching observation that the location of the zero  $(-1/T_{h1})$  is crucial in dictating the nature of the airplane's flight path behaviour.

Before going on to the design of the controller, it is worthwhile to try and understand the physics behind the strange behaviour of the flight path response. It becomes quite clear when one realises that flight path response is largely dependent upon the interplay of changes in lift and drag when the elevator is deflected. In this context it may be pointed out that during the approach phase, the airplane is operating on the left side of the 'drag vs. speed' curve .

Now we consider what happens when the elevator is deflected downward. The resulting nose-down moment causes decrease in the angle of attack with the attendant reduction in drag. This causes the airplane to accelerate as the airplane is operating at a speed below the minimum - drag speed. The resulting increase in speed leads to further reduction in drag which in turn causes the airplane to accelerate even more. The large gain in speed made possible through elevator deflection is accompanied by a corresponding hike in the lift, causing the flight path angle to

shift to a positive value. This reversal of hand is highly undesirable, it being the source of confusion to the pilot as pointed out earlier. It is thus apparent that in order to control the flight path at low Mach numbers, it is imperative to incorporate an additional speed control. The current practice thus involves providing such control either manually or through an autopilot.

We now direct our attention to the "all important" zero given by the constant  $(1/T_{h1})$ . This may be expressed as [3] :

$$\frac{1}{T_{h1}} = -X_u + (X_\alpha - g) \cdot \frac{Z_u \cdot (1 - Z_{\dot{\alpha}e} \cdot H_u / H_{\dot{\alpha}e} \cdot Z_u)}{Z_\alpha \cdot (1 - Z_{\dot{\alpha}e} \cdot H_\alpha / H_{\dot{\alpha}e} \cdot Z_\alpha)}$$

Thus this zero can be varied by changing the stability derivatives  $X_u$  and  $X_\alpha$ . Here the speed feedback control effectively augments the derivative  $X_u$ . This in turn changes the magnitude as well the sign of the zero  $(1/T_{h1})$ . This is precisely what is attempted in the design of the flight path controller.

**CHAPTER 3**  
**CONTROLLER SYNTHESIS**

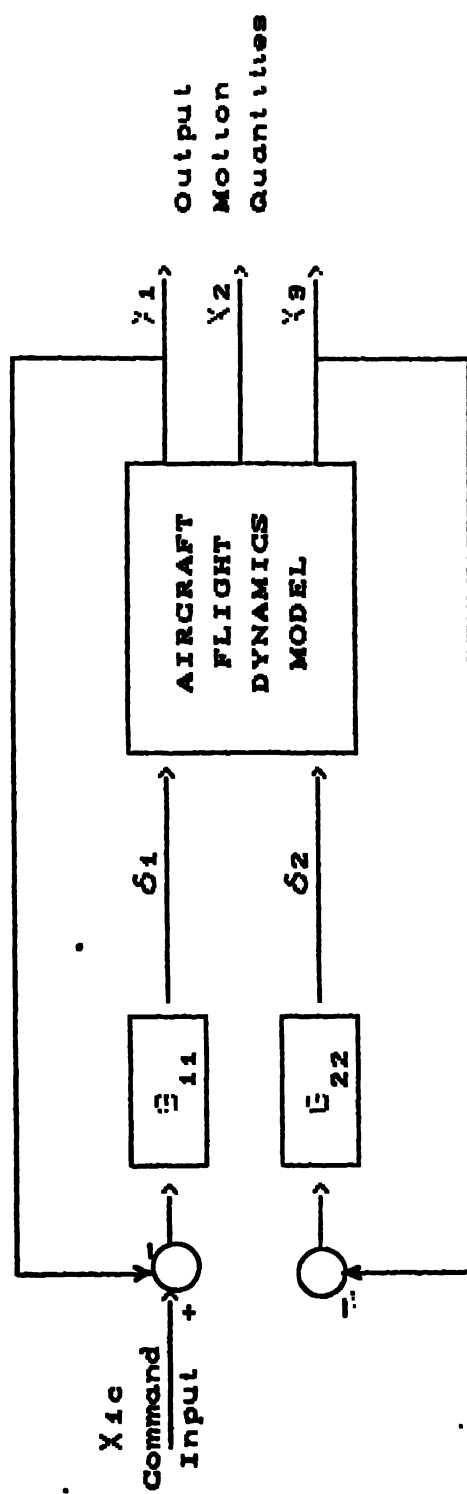


**Fig. 2 GENERAL STRUCTURE OF A MULTILoop FLIGHT CONTROL SYSTEM**

where :

$$A = \begin{bmatrix} a_{11} & a_{12} & a_{13} \\ a_{21} & a_{22} & a_{23} \\ a_{31} & a_{32} & a_{33} \end{bmatrix} ; B = \begin{bmatrix} b_{11} & b_{12} \\ b_{21} & b_{22} \\ b_{31} & b_{32} \end{bmatrix}$$

From (1) and (2) we get

$$A.X = B.(G_c.X_c - G.X) \quad \dots\dots(3)$$

$$\Rightarrow (A + BG).X = B.G_c.X_c \quad \dots\dots(4)$$

The corresponding characteristic polynomial of the closed loop system is

$$\Delta_{cl} = \det(A+BG) = \begin{vmatrix} a_{11} + b_{11}.G_{11} & a_{12} + b_{12}.G_{22} & a_{13} \\ a_{21} + b_{21}.G_{11} & a_{22} + b_{22}.G_{22} & a_{23} \\ a_{31} + b_{31}.G_{11} & a_{32} + b_{32}.G_{22} & a_{33} \end{vmatrix} \quad \dots(5)$$

On expanding this we get

$$\Delta_{cl} = \Delta_{ol} + G_{11}.N_{\delta_1}^{x1} + G_{22}.N_{\delta_2}^{x2} + G_{11}.G_{22}.N_{\delta_1 \delta_2}^{x1 \times 2} \quad \dots\dots(6)$$

where :

$\Delta_{ol}$  = system open loop characteristic polynomial =  $\det(A)$

$N_{\delta_1}^{x1}$  = numerator polynomial of the  $X_1$ -to- $\delta_1$  transfer function obtained by applying Cramer's Rule to (2)

$N_{\delta_2}^{x2}$  = numerator polynomial of the  $X_2$ -to- $\delta_2$  transfer function obtained by applying Cramer's Rule to (2)

$N_{\delta_1 \delta_2}^{x1 \times 2}$  is defined as the coupling numerator and is given by

$$N_{\delta_1 \delta_2}^{x1 \times 2} = \begin{vmatrix} b_{11} & b_{12} & a_{13} \\ b_{21} & b_{22} & a_{23} \\ b_{31} & b_{32} & a_{33} \end{vmatrix}$$

From (4) :

$$\begin{bmatrix} a_{11} + b_{11} \cdot G_{11} & a_{12} + b_{12} \cdot G_{22} & a_{13} \\ a_{21} + b_{21} \cdot G_{11} & a_{22} + b_{22} \cdot G_{22} & a_{23} \\ a_{31} + b_{31} \cdot G_{11} & a_{32} + b_{32} \cdot G_{22} & a_{33} \end{bmatrix} \begin{bmatrix} X_1 \\ X_2 \\ X_3 \end{bmatrix} = \begin{bmatrix} b_{11} \cdot G_{11} & b_{12} \cdot G_{22} \\ b_{21} \cdot G_{11} & b_{22} \cdot G_{22} \\ b_{31} \cdot G_{11} & b_{32} \cdot G_{22} \end{bmatrix} \begin{bmatrix} X_{10} \\ 0 \end{bmatrix} \quad \dots\dots(7)$$

Solving for  $X_1/X_{10}$ , the transfer function function of interest,

$$\begin{aligned} \frac{X_1}{X_{10}} &= \frac{\begin{vmatrix} b_{11} \cdot G_{11} & a_{12} + b_{12} \cdot G_{22} & a_{13} \\ b_{21} \cdot G_{11} & a_{22} + b_{22} \cdot G_{22} & a_{23} \\ b_{31} \cdot G_{11} & a_{32} + b_{32} \cdot G_{22} & a_{33} \end{vmatrix}}{\begin{vmatrix} a_{11} + b_{11} \cdot G_{11} & a_{12} + b_{12} \cdot G_{22} & a_{13} \\ a_{21} + b_{21} \cdot G_{11} & a_{22} + b_{22} \cdot G_{22} & a_{23} \\ a_{31} + b_{31} \cdot G_{11} & a_{32} + b_{32} \cdot G_{22} & a_{33} \end{vmatrix}} \\ &= \frac{G_{11} \cdot (N_{\delta 1}^{*1} + G_{22} \cdot N_{\delta 1}^{*1} \cdot x_2)}{\Delta_{o1} + G_{11} \cdot N_{\delta 1}^{*1} + G_{22} \cdot N_{\delta 2}^{*2} + G_{11} \cdot G_{22} \cdot N_{\delta 1}^{*1} \cdot x_2} \quad \dots(8) \end{aligned}$$

Dividing the numerator and the denominator by  $\Delta_{o1}$  and setting

$$N_{\delta 1}^{*1} / \Delta_{o1} = X_{1\delta 1}$$

$$N_{\delta 2}^{*2} / \Delta_{o1} = X_{2\delta 2}$$

we get,

$$\frac{X_1}{X_{10}} = \frac{G_{11} \cdot (X_{1\delta 1} + G_{22} \cdot N_{\delta 1}^{*1} \cdot x_2 \cdot X_{1\delta 1} / N_{\delta 1}^{*1})}{1 + G_{11} \cdot X_{1\delta 1} + G_{22} \cdot X_{2\delta 2} + G_{11} \cdot G_{22} \cdot N_{\delta 1}^{*1} \cdot x_2 \cdot X_{1\delta 1} / N_{\delta 1}^{*1}}$$

$$= \frac{G_{11} \cdot X_{1\delta_1} \cdot (1 + G_{22} \cdot N_{\delta_1 \delta_2}^{x1 \ x2} / N_{\delta_1}^{x1})}{1 + G_{22} \cdot X_{2\delta_2} + \{G_{11} \cdot X_{1\delta_1} \cdot (1 + G_{22} \cdot N_{\delta_1 \delta_2}^{x1 \ x2} / N_{\delta_1}^{x1})\}} \dots\dots(9)$$

Note that this can be put in the form  $G/(1 + G)$ . For this unity feedback closed loop system, the corresponding open loop system simply becomes  $G$ , given by :

$$G = \frac{G_{11} \cdot X_{1\delta_1} \cdot (1 + G_{22} \cdot N_{\delta_1 \delta_2}^{x1 \ x2} / N_{\delta_1}^{x1})}{(1 + G_{22} \cdot X_{2\delta_2})} = G_{11} \cdot X_{1\delta_1}' \dots\dots(10)$$

Fig.3 shows how the open loop  $X_{1\delta_1}$  transfer function has been modified by the two factors  $(1 + G_{22} \cdot N_{\delta_1 \delta_2}^{x1 \ x2} / N_{\delta_1}^{x1})$  and  $\{1 / (1 + G_{22} \cdot X_{2\delta_2})\}$  as a result of closing only the  $X_2$ -to- $\delta_2$  loop. The new  $X_1$ -to- $\delta_1$  transfer function,  $X_{1\delta_1}'$ , can be rewritten as :

$$\begin{aligned} X_{1\delta_1}' &= \frac{X_{1\delta_1} \cdot (1 + G_{22} \cdot N_{\delta_1 \delta_2}^{x1 \ x2} / N_{\delta_1}^{x1})}{(1 + G_{22} \cdot X_{2\delta_2})} \\ &= \frac{(N_{\delta_1}^{x1} + G_{22} \cdot N_{\delta_1 \delta_2}^{x1 \ x2})}{(\Delta_{o1} + G_{22} \cdot N_{\delta_2}^{x2})} \dots\dots(11) \end{aligned}$$

It so turns out that the zeros and poles of  $X_{1\delta_1}'$  correspond to the characteristic roots of the two rather simple unity feedback systems shown in Fig. 4a and Fig. 4b respectively. The closed loop transfer functions of these two loops are, respectively :

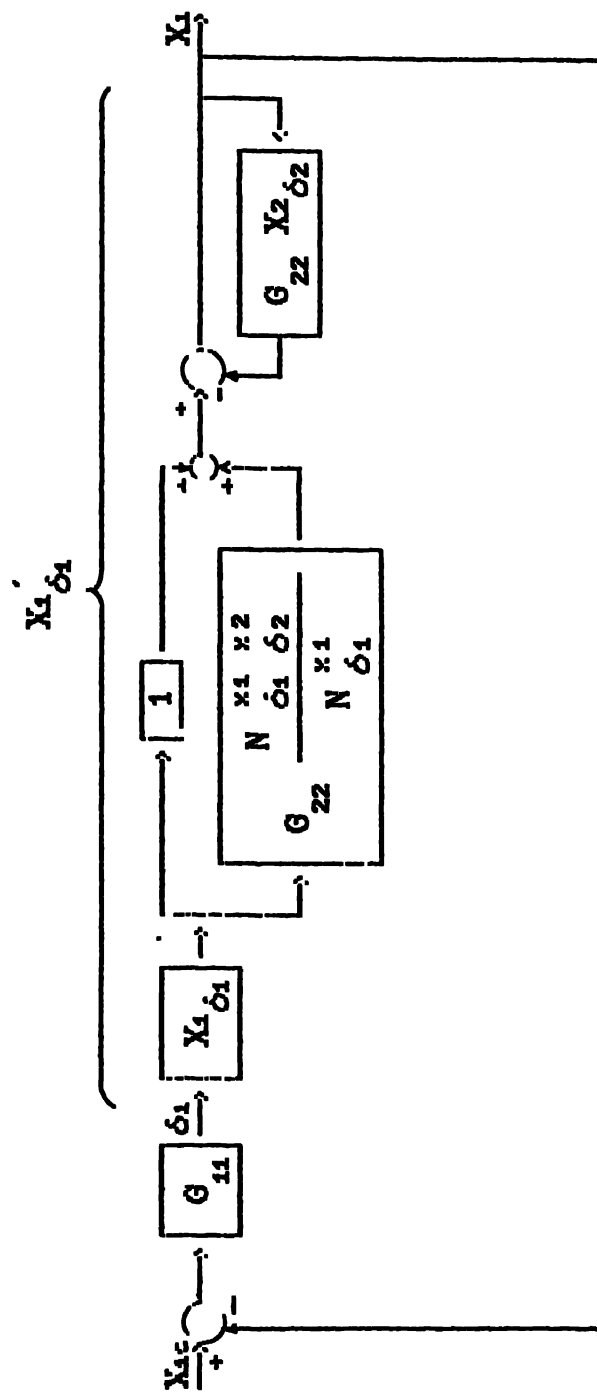


**Fig.3 Equivalent Block Diagram of the system :  $X_1 \rightarrow \delta_1, X_2 \rightarrow \delta_2$**



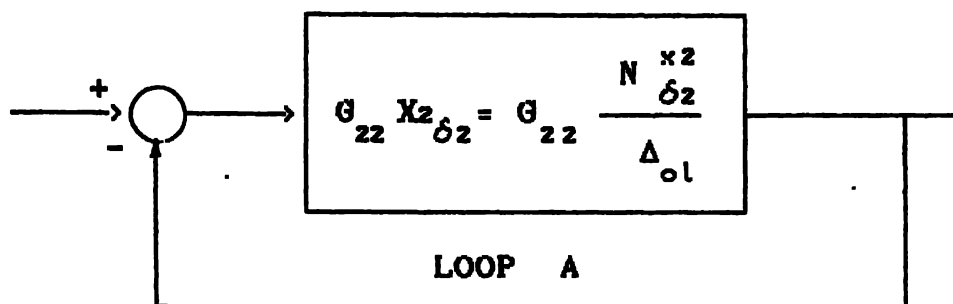


Fig. 4 a

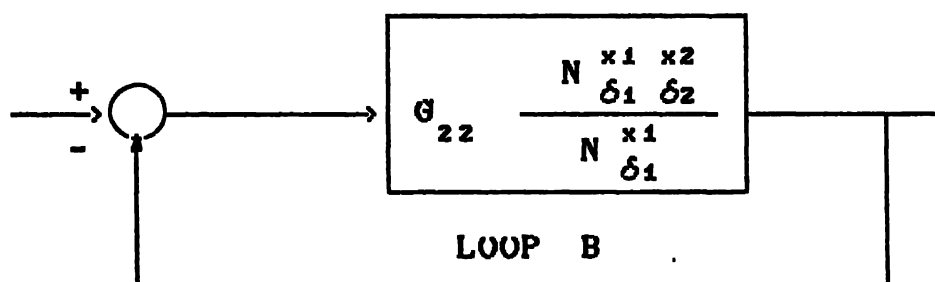


Fig. 4 b

Fig. 4 Equivalent Sub-systems of the system :  $X_2 \rightarrow \delta_2$

City: KANPUR  
 I. T. KANPUR  
 No. A. 117672

$$\frac{G_{22} \cdot N_{\delta 2}^{x2}}{\Delta_{ol} + G_{22} \cdot N_{\delta 2}^{x2}} \quad \text{and} \quad \frac{G_{22} \cdot N_{\delta 1}^{x1} \cdot x2}{N_{\delta 1}^{x1} + G_{22} \cdot N_{\delta 1}^{x1} \cdot x2}$$

The above observation is of crucial significance as the poles as well as the zeros of  $X_{1\delta_1}$  can now be regulated by the root-locus design of these two "feedback sub-systems". The suitable choice of  $G_{22}$  now enables us to proceed with the final step of synthesizing  $G_{11}$ . Obviously this compensator must be chosen so as to ensure the required overall system performance.

#### APPLICATION OF THE PROPOSED DESIGN APPROACH

The variables used in the synthesis are as follows :

$$X = \begin{bmatrix} X_1 \\ X_2 \\ X_3 \end{bmatrix} = \begin{bmatrix} \gamma \\ u / \Pi \\ \alpha \end{bmatrix} ; \quad \delta = \begin{bmatrix} \delta_{ab} \\ \delta_e \end{bmatrix}$$

Since the primary objective is to control flight path, it is chosen to the 'outer' feedback loop and speed ( $u$ ) is chosen to form the 'inner' loop.

The main problem being the non-minimum phase zero  $-1/T_{h1}$ , we first try to place the zeros of the outer flight path loop by designing the closure of the coupling Loop B, since the closed loop poles of this one are the very open loop zeros of the outer loop. Also, since the numerator of the corresponding open loop transfer function i.e., the coupling numerator, has one non-minimum phase zero, naturally it is essential that this loop

have no open loop poles in the right half plane. In other words, we need to select  $N_{\delta_1}^{x1}$  so that it has no non-minimum phase zeros. The only choice available is the numerator of the  $\gamma$ -to- $\delta_{ab}$  transfer function, and this fixes the choice of the two feedbacks.

#### DESIGN DATA

The following design data is assumed for a generic delta-winged high performance fighter flying at sea level at  $M = 0.2$ ,  $\gamma = -2$  deg :

$$\begin{aligned} Z_{\alpha} / U &= -0.5146 ; g \cdot \sin \gamma_o = -0.0050 ; Z_u = -0.2670 \\ M_{\alpha} &= -0.87 ; M_q = -1.85 ; M_u \cdot U = 0.1960 \\ X_{\alpha} / U &= -0.1459 ; g \cdot \cos \gamma_o = 0.1441 ; X_u = -0.0765 \\ Z_{\delta_e} / U &= -0.1453 ; Z_{\delta_{ab}} / U = 0.0001 ; M_{\delta_e} = -3.0550 \\ M_{\delta_{ab}} &= -0.0015 ; X_{\delta_e} / U = -0.0166 ; X_{\delta_{ab}} / U = -0.0506 \end{aligned}$$

The equations of motion of the aircraft are :

$$\begin{bmatrix} -M_u \cdot U & s^2 - M_q s - M_{\alpha} & s^2 - M_q s \\ s - X_u & \frac{(-X_{\alpha} + g \cdot \cos \gamma)}{U} & \frac{g \cdot \cos \gamma}{U} \\ -Z_u & \frac{(s - Z_{\alpha} + g \cdot \sin \gamma)}{U} & \frac{(g \cdot \sin \gamma - s)}{U} \end{bmatrix} \begin{bmatrix} \gamma \\ \frac{u}{U} \\ \alpha \end{bmatrix} = \begin{bmatrix} M_{\delta_{ab}} & M_{\delta_{at}} \\ \frac{X_{\delta_{ab}}}{U} & \frac{X_{\delta_{at}}}{U} \\ \frac{Z_{\delta_{ab}}}{U} & \frac{Z_{\delta_{at}}}{U} \end{bmatrix} \begin{bmatrix} \delta_{ab} \\ \delta_{at} \end{bmatrix}$$

Here the state vector comprises of the dimensionless forward velocity, the angle of attack and the flight path angle (instead of the pitch attitude angle normally used).

Applying Cramer's Rule to the equations of motion we have the following :

1) The open loop characteristic polynomial i.e., the denominator of the transfer functions is

$$\begin{aligned}\Delta_{o1} &= s^4 + 2.4411.s^3 + 1.9639.s^2 + 0.1292.s + 0.0486 \\ &= [s^2 + 2(0.88)(1.36)s + (1.36)^2][s^2 + 2(0.11)(0.16)s + (0.16)^2]\end{aligned}$$

$$\begin{aligned}2) \frac{u}{\delta_e} &= \frac{N_{\delta_e}^u}{\Delta_{o1}} = \frac{-0.0466 s^3 - 0.0889 s^2 + 0.8403 s + 0.2104}{\Delta_{o1}} \\ &= \frac{-0.0046 (s - 3.5424).(s + 0.2449).(s + 5.2053)}{\Delta_{o1}}\end{aligned}$$

$$\begin{aligned}3) \frac{\gamma}{\delta_e} &= \frac{N_{\delta_e}^\gamma}{\Delta_{o1}} = \frac{0.1453 s^3 + 0.2675 s^2 - 1.4328 s + 0.1200}{\Delta_{o1}} \\ &= \frac{0.1453 (s - 0.0852).(s - 2.2964).(s + 4.2226)}{\Delta_{o1}}\end{aligned}$$

$$\begin{aligned}4) \frac{u}{\delta_{ab}} &= \frac{N_{\delta_{ab}}^u}{\Delta_{o1}} = \frac{0.0506 s^3 - 0.1197 s^2 - 0.0918 s - 0.0001}{\Delta_{o1}} \\ &= \frac{0.0506 (s + 0.0011).[s^2 + 2(0.88)(1.35)s + (1.35)^2]}{\Delta_{o1}}\end{aligned}$$

$$\begin{aligned}5) \frac{\gamma}{\delta_{ab}} &= \frac{N_{\delta_{ab}}^\gamma}{\Delta_{o1}} = \frac{-0.0001 s^3 - 0.0136 s^2 - 0.0258 s - 0.0168}{\Delta_{o1}} \\ &= \frac{-0.0001(s + 135.12).[s^2 + 2(0.86)(1.12)s + (1.12)^2]}{\Delta_{o1}}\end{aligned}$$

6) The coupling numerator is given by :

$$\begin{aligned} N_{\delta_{ab}}^{\gamma} \delta_e^u &= 0.0074 s^2 + 0.0136 s - 0.0725 \\ &= 0.0074 (s + 4.1824)(s - 2.3446) \end{aligned}$$

### DESIGN

Since the placement of the outer-loop zeros is of paramount importance, as also explained earlier, we begin by designing the coupling loop first. The root locus technique is utilized here for the design.

For the data assumed, the open loop transfer function of the coupling loop can be written as

$$\frac{N_{\delta_{ab}}^{\gamma} \delta_e^u}{N_{\delta_{ab}}^{\gamma}} = \frac{0.0074 s^2 + 0.0136 s - 0.0725}{-0.0001 s^3 - 0.0136 s^2 - 0.0258 s - 0.0168}$$

Fig.5 shows the root locus plot for this transfer function. As can be seen, the presence of the non-minimum phase zero at +2.3 tends to draw the root locus into the right half plane even for low values of gain. This will clearly not suit our purpose. Hence we try to remedy this by selecting a compensator that will pull the poles to the left when the loop is closed. This required several trials, however. It was found that using the lead compensator

$$G_{22} = \frac{(s + 1.5)}{(s + 6)}$$

accomplishes the desired task suitably.

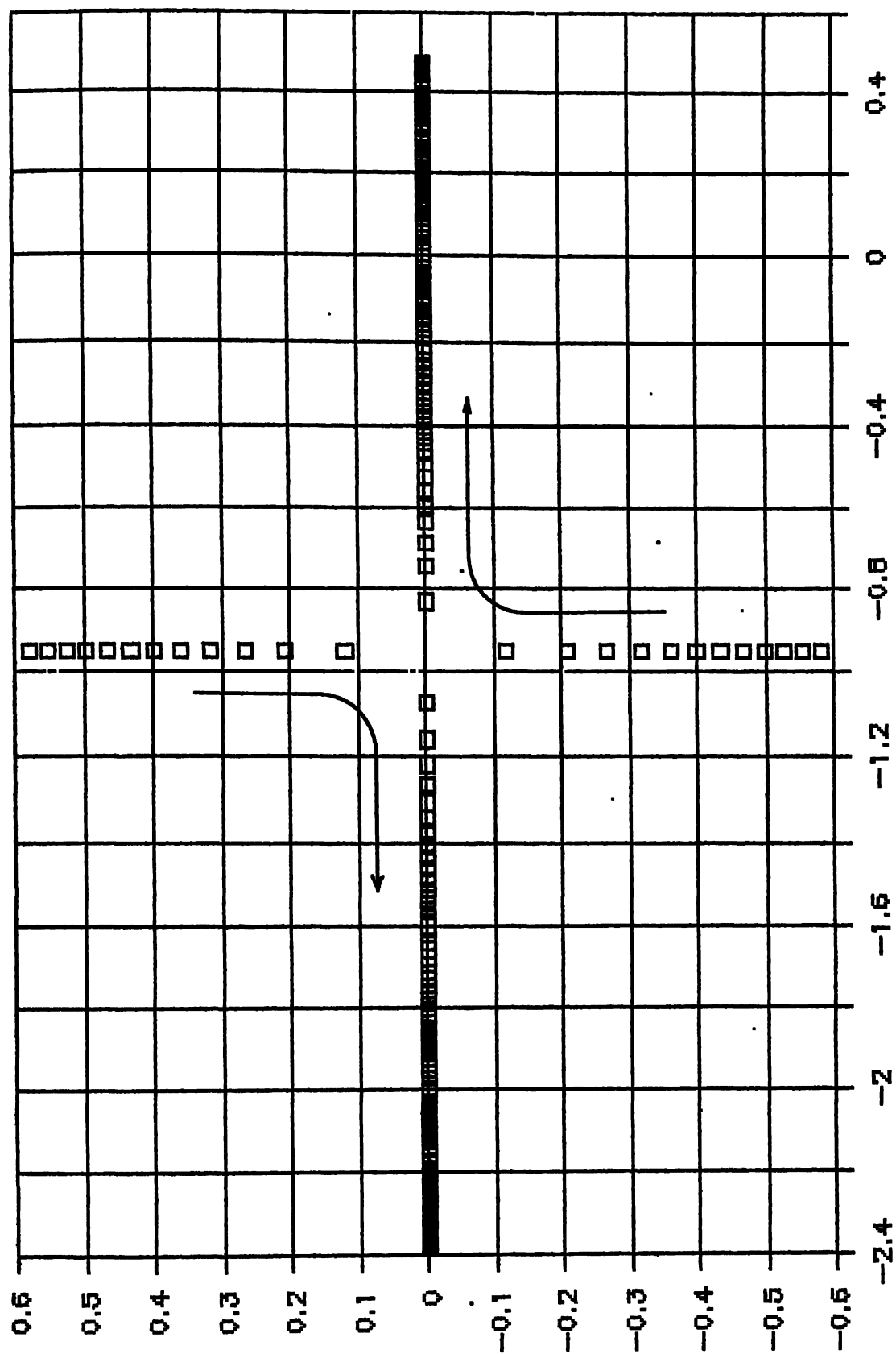


Fig.6 Root locus of the Coupling Loop B  
(with lead compensator)

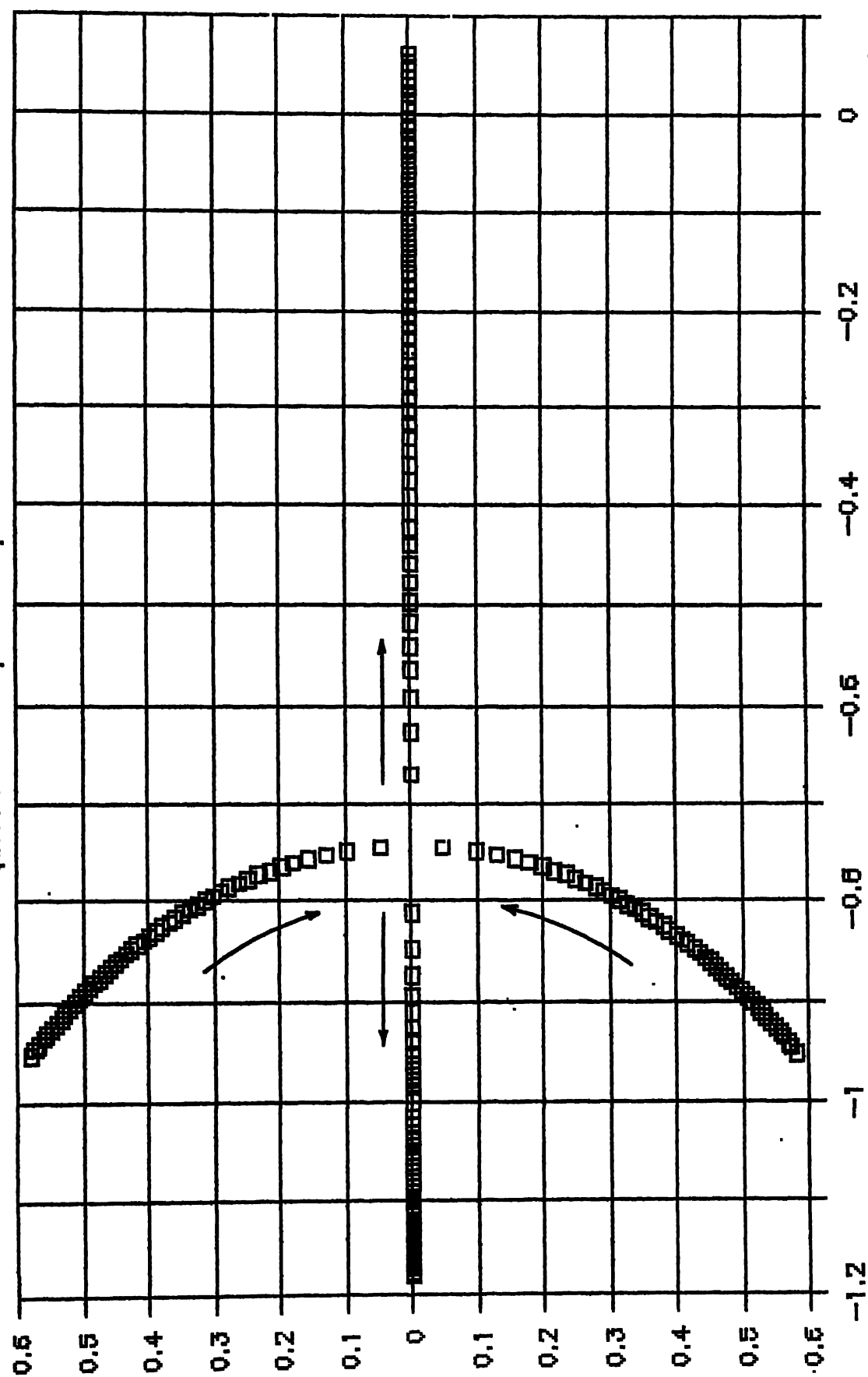


Fig. 6 shows the root locus plot with this compensator in the loop. Selecting a gain of 0.3 we obtain the following closed loop poles :

$$-0.8082 \pm 0.3378 i ; -5.6364 ; -157.85.$$

It may be noted that since none of these is in the right half plane, our outer loop transfer function will have no non-minimum phase zeros.

With the compensator now chosen, the inner loop A is closed. For this loop the open loop transfer function can be stated as :

$$\frac{N_{\Delta_{ol}}^u}{\Delta_{ol}} = \frac{-0.0466 s^3 - 0.0889 s^2 + 0.8403 s + 0.2104}{s^4 + 2.4411 s^3 + 1.9639 s^2 + 0.1292 s + 0.0486}$$

The root locus plot for this transfer function is shown in Fig. 7 and the closed loop poles for the gain  $k = 0.30$  are :

$$-6.0033; -1.2217 \pm 0.6396i ; -0.0042 \pm 0.1313i.$$

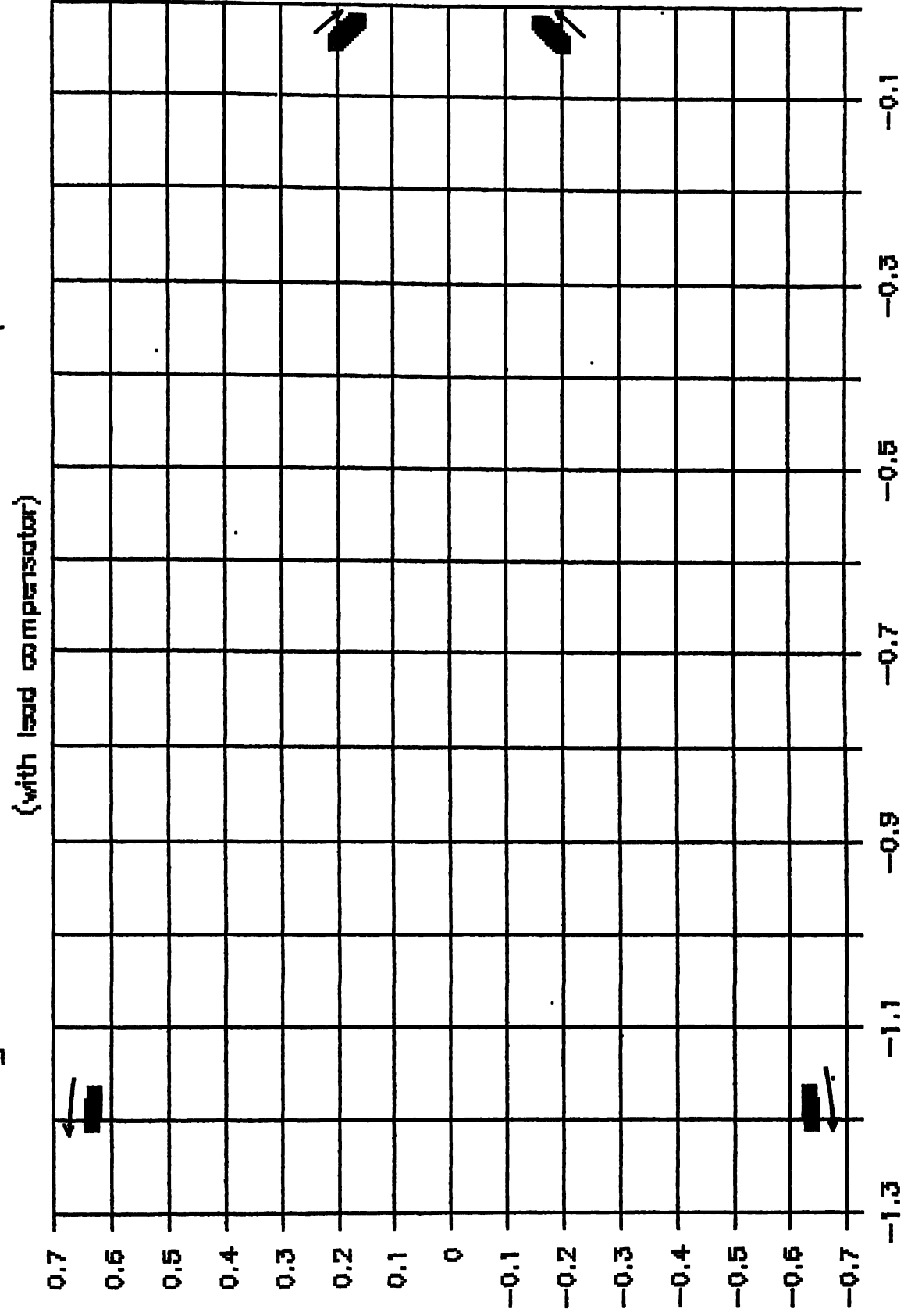
These are the open loop poles of the outer loop.

Having placed the open loop poles and zeros for the flight path loop, we now focus on designing the closure of the outer loop. This is done using the 'connect' function of the MATLAB software package which allows us to handle the multi-input-multi-output system at hand. The open loop transfer function of the outer loop obtained is :

$$\frac{-0.0001s^4 - 0.0185s^3 - 0.1155s^2 - 0.1563s - 0.0683}{s^5 + 8.455 s^4 + 16.66 s^3 + 11.70 s^2 + 0.392 s + 0.187}$$



Fig.7 Root Locus of Inner Loop A



$$= \frac{-0.0001(s + 157.85)(s + 5.6334)}{(s + 6.003)[s^2 + 2(0.89)(1.38)s + (1.38)^2]} + \frac{[s^2 + 2(0.92)(0.88)s + (0.88)^2]}{[s^2 + 2(0.03)(0.13)s + (0.13)^2]}$$

and this clearly checks with the poles and zeros assigned.

Fig. 8 shows the root locus plot for the overall HMM feedback control system resulting from the closure of this loop. We select the gain  $k = 9$  to ensure adequate phugoid damping.

The response of this closed loop system to a unit step  $\gamma$  command is plotted in Fig.9. We also obtain the response of the other important flight variable, airspeed, to the same input. (Fig.10).

It may be observed that while the airspeed fluctuations eventually vanish as required, they do so after going through a number of slow oscillations. It is therefore essential to go through another iterative attempt at designing the outer loop closure with a view to achieving quick decay of the airspeed fluctuations.

It is obvious that the long decay time exhibited by the airspeed response is a manifestation of the phugoid dynamics with its characteristic low frequency oscillation. The surest way to reduce the decay time would be to use a compensator that nullifies the effect of the phugoid poles. Hence after a few trials, a second

Fig.8 Root locus of Flight Path Loop

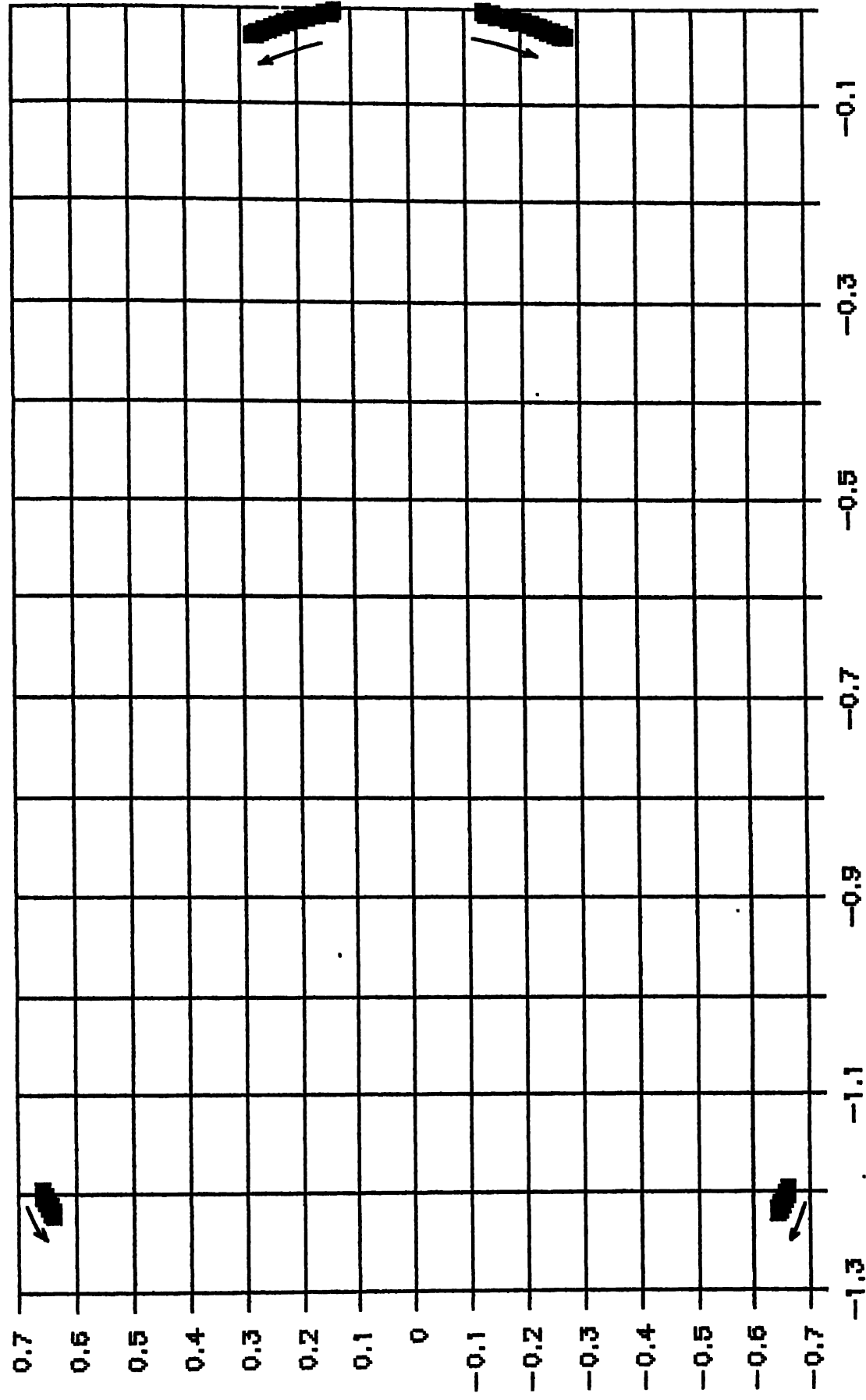


Fig.9 Gamma Resp. to Gamma command

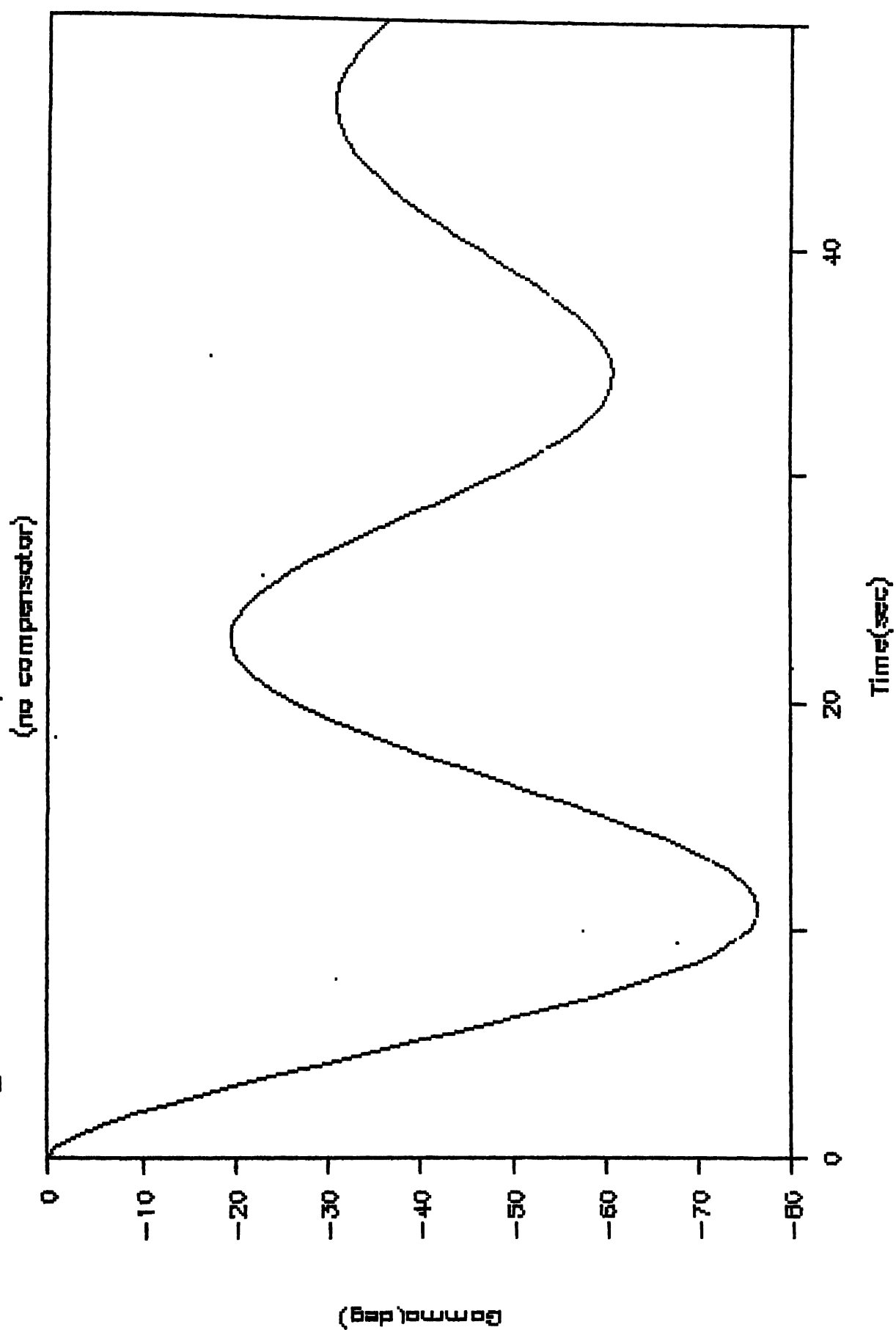
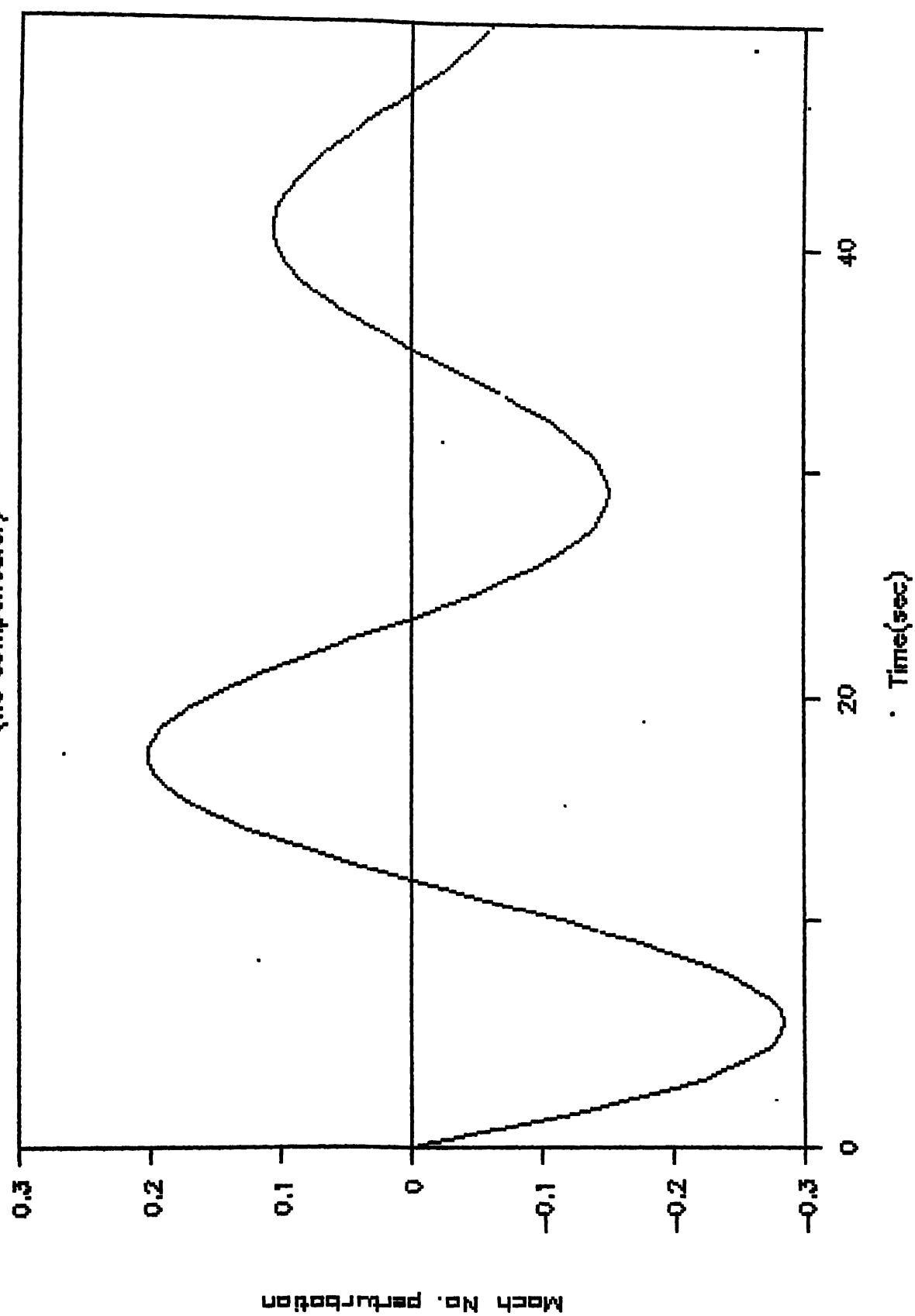


Fig.10 Airspeed resp. to gamma command  
(no compensator)



order compensator is selected with

$$G_{11} = \frac{(s^2 + 0.0004 s + 0.0175)}{s^2 + 3.5 s + 3}$$

To check the improvement in the system performance, the time responses are again studied for unit step inputs to  $(r/\gamma_c)$  and  $(u/\gamma_c)$ . These are plotted in Fig.11 and Fig.12 respectively. The remarkable effect of the compensator on the outer loop response is immediately apparent.

Fig.11 Gamma resp. to Gamma command  
(With compensator)

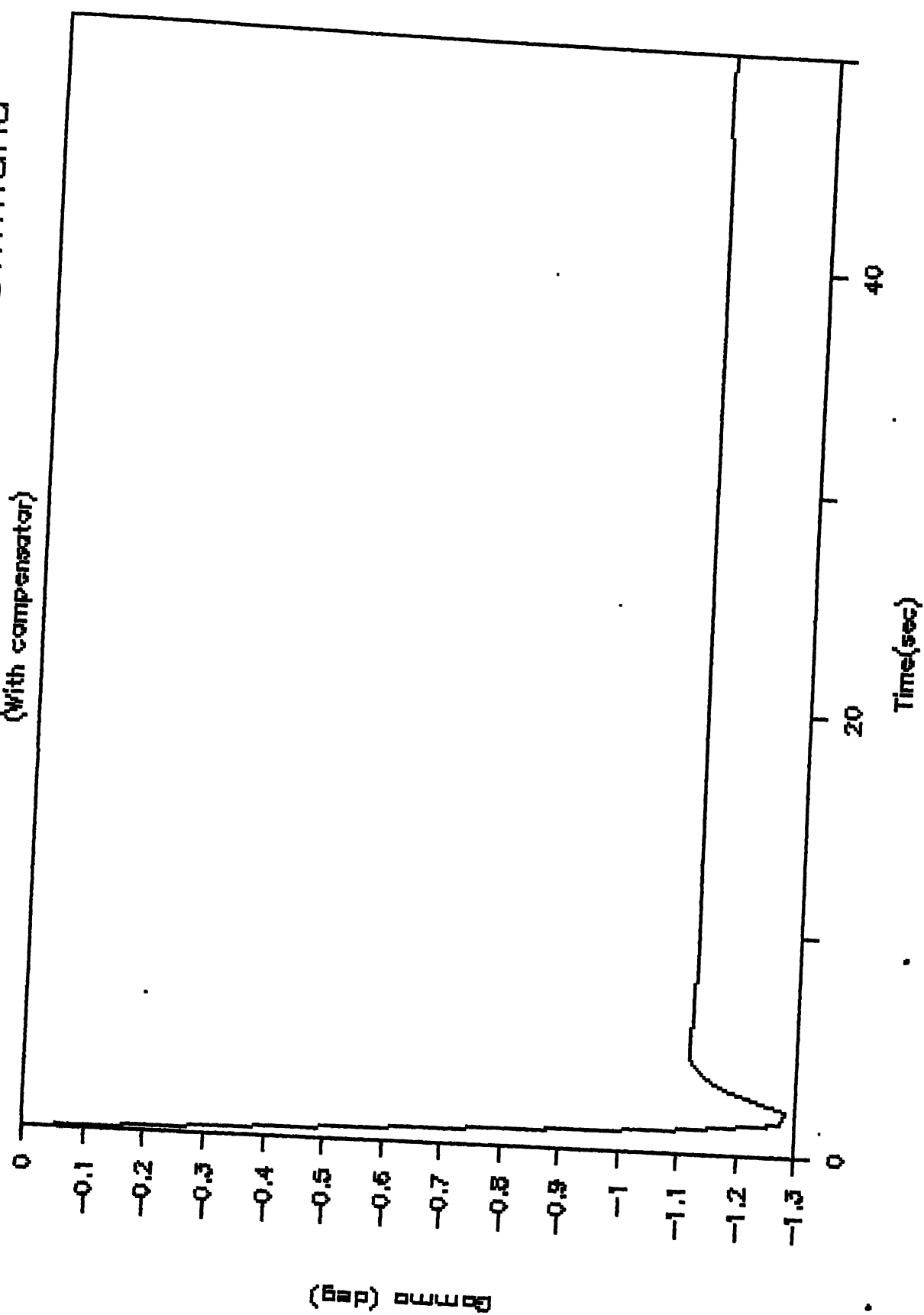
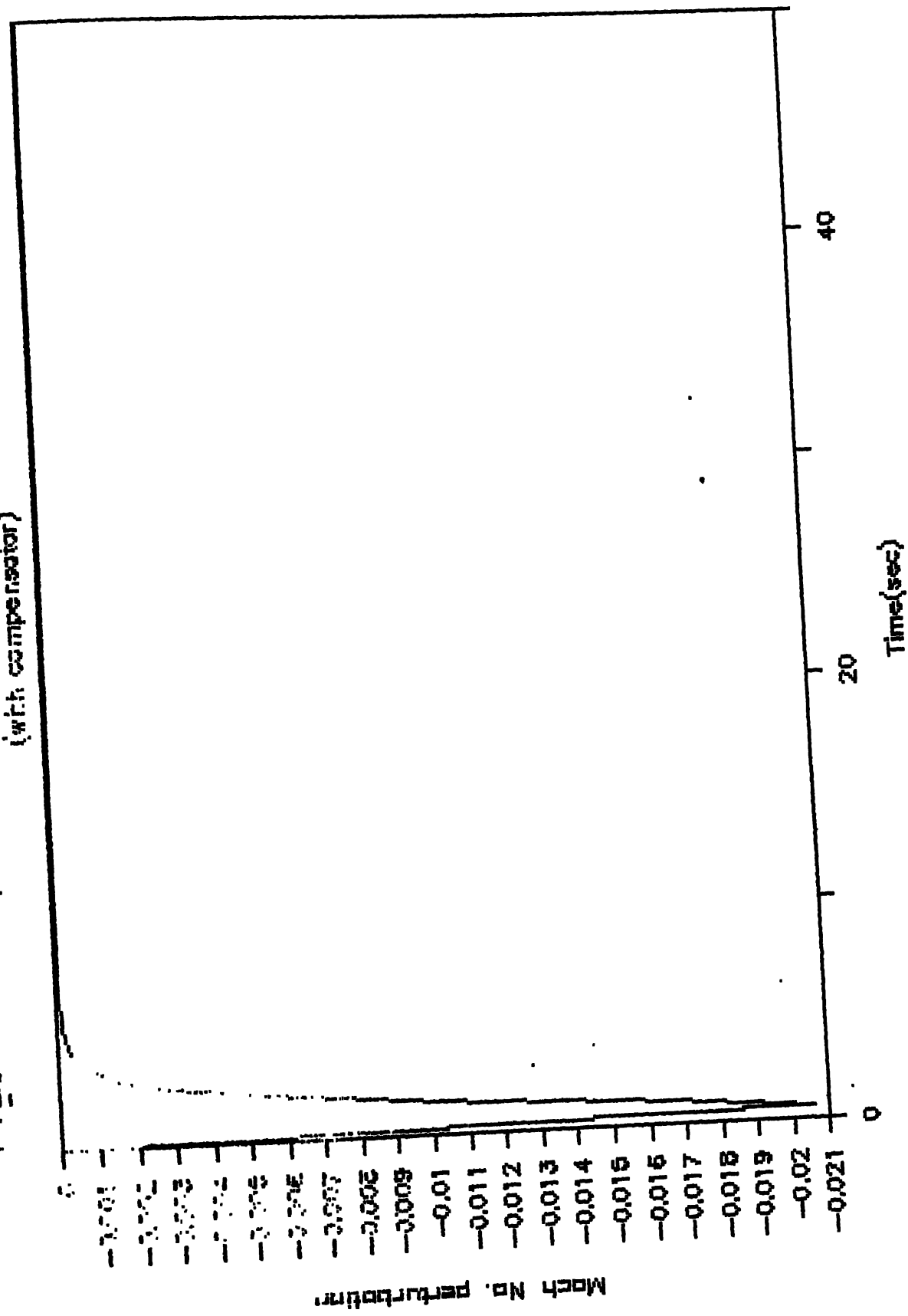


Fig. 12 Airspeed resp. to gamma command  
(with compensator)





## CHAPTER 4

## RESULTS AND CONCLUSIONS

As can be seen from Fig. 11 illustrating the controller effectiveness, a positive step input through the airbrakes results in a negative steady state flight path angle. This implies that extending the airbrakes now results in a steady rate of descent. In addition there is no hint of a non - minimum phase behaviour and the plot shows a well damped crisp response.

The airspeed response for the same step input is presented in Fig. 12. Evidently there is a "small" drop in the forward airspeed before it is quickly neutralised as the airplane descends and accelerates. However when the steady state is attained, there is no subsequent change in the airspeed. It may be emphasised that the resulting change in the airspeed observed is fairly small. Here, the change in the flight path angle by as much as 1 deg. results in a change in the airspeed by less than 0.02 M which happens to be insignificant even at the low speeds of the approach.

Thus, the desired objective of rectifying the anomalous flight path response at low speeds has been achieved. Furthermore, the control synthesis enables decoupling the flight path from the airspeed. The importance of this cannot be overemphasised. It is now possible to select the airspeed before engaging the controller for approach. In view of the decoupling achieved and with the desired airspeed already attained, the pilot no longer has to

worry about the airspeed fluctuations. Thus, the pilot is free to control his flight path with virtually no concern regarding any undue changes in the trimmed airspeed. This is clearly a much simpler procedure than the established one of continuously juggling the throttle and the stick.

#### CONCLUSIONS

A novel approach at flight path control has been attempted to facilitate airplane handling during the landing approach. Initial emphasis was laid on theoretically establishing as to why the zero ( $-1/T_{h1}$ ) in the flight path - to - elevator transfer function is considered as the parameter of prime importance. The conceptual clarity achieved in the process proved to be of considerable importance in the controller synthesis. It was realized that the placement of this zero has to be regulated to ensure its location in the left half s-plane with an overall view of achieving the desired flight path control. With the simple root locus design concept, applied here to a multi - input - multi - output system, it has been possible to achieve this broad objective commendably.

#### RECOMMENDATIONS FOR FURTHER WORK

The present design is simplistic in nature as it applies to a specific landing speed. It needs to be extended for general applications covering landing over a range of Mach numbers. Besides, the effects of gusts have not been considered. These must be studied carefully as gusts have long been the bane of pilots during the landing approach as well as the flare - and - touchdown maneuver. Finally, the effects of including the airbrakes

actuator must also be examined.

One can envisage a complete flight path controller that totally decouples flight path and airspeed from each other and includes all landing phases including flare and touchdown.

## REFERENCES :

1. John H. Blakelock , *Automatic Control of Aircraft and Missiles*, John Wiley and Sons. 1965.
2. Jan Roskam. *Airplane Flight Dynamics and Automatic Flight Controls. Part 2*. Roskam Aviation and Engineering Corporation, 1977.
3. Daniel F. McIver, Irving Ashkenas and Dunstan Graham, *Aircraft Dynamics and Automatic Control*. Princeton University Press, 1973.
4. Brian L. Stevens and Frank L. Lewis, *Aircraft Simulation and Control*. John Wiley and Sons, 1992.
5. Herman F. Fortmann and Konrad L. Hitz, *An Introduction to Linear Control Systems*. Marcel Dekker Inc., 1977.
6. Howard L. Harrison and John G. Hollinger, *Introduction to Automatic Controls*. International Textbook Co., 1968.